

# C 80-113

## Deflection of a Near-Vertical Towing Cable in a Nonuniform Flowfield

00001  
00018  
00021

N. E. Gilbert\*

*Aeronautical Research Laboratories, Department of Defence, Melbourne, Australia*

A three-dimensional steady-state mathematical model of a cable used to suspend a sonar body from a helicopter is derived. Two-dimensional "power" and "log" laws are assumed for the wind above the sea, and a three-dimensional Ekman spiral is assumed for the sea current. Solutions are obtained in dimensionless form for a length of cable totally immersed in any Newtonian fluid, and may therefore be applied to a number of practical cable problems. Various approximations are made in order to obtain an analytical solution for a uniform fluid velocity. For nonuniform fluid velocities, a procedure is developed whereby the velocity function is replaced by an equivalent mean value in order that the "approximate" analytical solution for a uniform fluid velocity may be used.

### Nomenclature

$c$	$= 1 + h/h_o$
$C_D$	$=$ drag coefficient of cable in the lateral direction of flow
$d$	$=$ depth of frictional resistance
$d_c$	$=$ cable diameter
$D, H$	$= d/z_l$ and $h/z_l$
$g$	$=$ gravitational acceleration (along $z_E$ axis)
$h$	$=$ height of $P_o$ above the sea (i.e., hover height)
$h_o$	$=$ surface roughness length
$k_c$	$= \frac{1}{2} \rho_F d_c C_D$
$m$	$=$ effective cable mass per unit length (allowing for buoyancy effect)
$n$	$=$ positive integer
$P$	$=$ upper end of cable element
$P_o, P_l$	$=$ upper and lower ends of cable length
$s$	$=$ distance of $P$ from $P_o$ along cable
$T$	$=$ tension force at $P$
$u^*$	$=$ velocity magnitude of fluid relative to cable
$U^*$	$=$ nondimensional velocity magnitude $(k_c z_l / T_l)^{1/2} u^*$
$u_F^* u_H^*$	$=$ velocity magnitude of fluid and cable relative to Earth
$u_F, v_F$	$=$ $x$ and $y$ components of fluid velocity in Earth axes
$u_H, v_H$	$=$ $x$ and $y$ components of cable velocity in Earth axes
$u, v, w$	$=$ $x, y$ , and $z$ components of velocity of fluid relative to cable
$U, V$	$=$ $x$ and $y$ components of $U^*$
$x_E, y_E, z_E$	$=$ Earth axes (coincide momentarily with cable axes)
$x_s, y_s, z_s$	$=$ cable element axes (see Fig. 1)
$xyz$	$=$ cable axes (see Fig. 1)
$x, y, z$	$=$ linear displacement components of $P$ in cable axes
$X, Y, Z, S$	$=$ $x/z_l, y/z_l, z/z_l$ , and $s/z_l$
$\alpha, \beta, \gamma$	$=$ direction cosine angles of cable element axes with respect to cable axes

$\beta x, \beta y$	$= \int_0^l U^* U dZ$ and $\int_0^l U^* V dZ$
$\delta$	$=$ increment in quantity prefixed
$\theta, \phi$	$=$ pitch and roll Euler angles when rotating $xyz$ axes to $x_s, y_s, z_s$ axes (pitch followed by roll)
$\lambda, \sigma, \omega$	$= U_H^*/U_{F0}^*, U^*/U_{F0}^*$ , and $U_F^*/U_{F0}^*$ ( $x, y$ components given by subscript $x$ and $y$ )
$\mu$	$= mg z_l / T_l$
$\rho_F$	$=$ fluid density
$\phi_E$	$=$ geographical latitude
$\chi, \gamma$	$=$ yaw and pitch Euler angles when rotating $xyz$ axes to $x_s, y_s, z_s$ axes (yaw followed by pitch)
$\psi$	$=$ velocity direction of fluid relative to cable
$\psi_F, \psi_H$	$=$ velocity direction of fluid and cable
$< >$	$=$ enclosed quantity is a mean value

### Subscripts

$A, W$	$=$ replaces subscript $F$ when the fluid is air, water
$s$	$=$ quantity is in cable element axes
$0, l$	$=$ value at $P_o, P_l$ (may follow other subscripts)

### Introduction

FOR the underwater detection of submarines, helicopters commonly use a sonar body which is lowered into the water by cable. For efficient operation of the system, it is generally important for the sonar body to remain as close to the vertical as possible while submerged. For a calm sea with little or no wind, this is achieved by maneuvering the helicopter, either manually or automatically via the helicopter control system, in such a way that the cable deviations (in pitch and roll) from the vertical at the suspension point are kept close to zero. For the case of a steady nonzero wind, resulting cable bow requires one or both of these angular deviations to be kept constant at nonzero values. A mathematical model of the cable and sonar body enables these angles, which are referred to as offset cable angle corrections, to be estimated, and allows an investigation of the behavior of the system under certain conditions.

A three-dimensional, time-dependent model in which the cable is represented by a number of rigid links is described in Ref. 1. However, it is sufficient, and considerably more

Received July 9, 1979; revision received Nov. 8, 1979. Copyright © American Institute of Aeronautics and Astronautics, Inc., 1979. All rights reserved.

Index categories: Aerodynamics; Helicopters; Military Missions.

\*Research Scientist, Aerodynamics Division.

convenient, to consider a steady-state model to investigate much of the behavior of the system. This applied particularly to the problem of calculating the offset cable angle corrections, which need to be assumed invariant with time. The treatment ignores the sea waves which would cause nonsteady effects, including cable oscillation. Steady-state solutions have been presented by other authors,<sup>2-6</sup> but are restricted to two-dimensional motion in a uniform flowfield. These restrictions are removed in this document. Formulae and results are presented in dimensionless form for a length of cable totally immersed in any Newtonian fluid, and may therefore be applied to a number of cable problems.

Solutions to the general equilibrium equations giving cable orientation at the top end of the cable are first obtained. Various approximations are then made which allow an analytical solution for a uniform fluid velocity. The suitability of the approximations is investigated by parameter studies in which solutions of the general and approximate equations are compared. Assuming these approximations, it is shown that a nonuniform fluid velocity may be replaced by an equivalent mean value in order that the uniform fluid velocity analytical solution may be used. This concept is also of use in developing a mathematical model for a flight simulator, where it is important to simplify the representation of the environment as much as possible. Equivalent mean fluid velocities are presented for typical wind and sea velocity profiles. These include two-dimensional "power" and "log" laws for the wind above the sea, and a three-dimensional Ekman spiral for the sea current. Finally, an example is given that is typical of a sonar body suspended from a helicopter.

### Mathematical Model

In order to investigate the behavior of a cable used to suspend a sonar body from a helicopter, the following steady-state mathematical model is formulated. Given the tension and angular orientation of the cable at the attached body, the angular orientation of the cable at the helicopter is required for any given steady-state relative motion between the helicopter and the air and sea. When the body is submerged, a solution is first obtained for the length of cable also submerged. This solution then provides the necessary boundary conditions for the solution for the length of cable above the sea.

Consider a length of cable totally immersed in a Newtonian fluid with the fluid moving horizontally. It is assumed that the only forces acting on the cable are the tension force, effective gravitational force (i.e., including buoyancy effect), and fluid drag force normal to the cable. Effects of cable twist, skin friction, induced mass, and elasticity of the cable are not considered here. The tension force and angular orientation at  $P_1$ , the lower end of the cable length, are assumed given and the angular orientation at  $P_0$ , the upper end of the cable length, is required. Since the relative motion is steady state, the gravitational, fluid, and tension forces acting on an element of length  $\delta s$  at  $P$  are in equilibrium (see Fig. 1). To resolve these forces in cable element axes, angular orientation of the cable element axes relative to the cable axes is expressed in terms of the conventional Euler angles used in aircraft aerodynamics where the order of rotation is yaw, pitch, and roll. However, because the effects of cable twist are ignored, only two angles are required to define the orientation. To avoid singularities, pitch and roll angles  $\theta$  and  $\phi$  are mostly used; in some instances, however, it is convenient to use angles obtained by a rotation in yaw  $\chi$ , followed by pitch  $\gamma$ . The angles may be related to  $\theta$  and  $\phi$  by considering the direction cosines of the cable element axes with respect to the cable axes. The direction cosines are given by Duncan<sup>7</sup> as

$$\cos \alpha = dx/ds = \sin \theta \cos \phi \quad (1a)$$

$$\cos \beta = dy/ds = -\sin \phi \quad (1b)$$

$$\cos \gamma = dz/ds = \cos \theta \cos \phi \quad (1c)$$

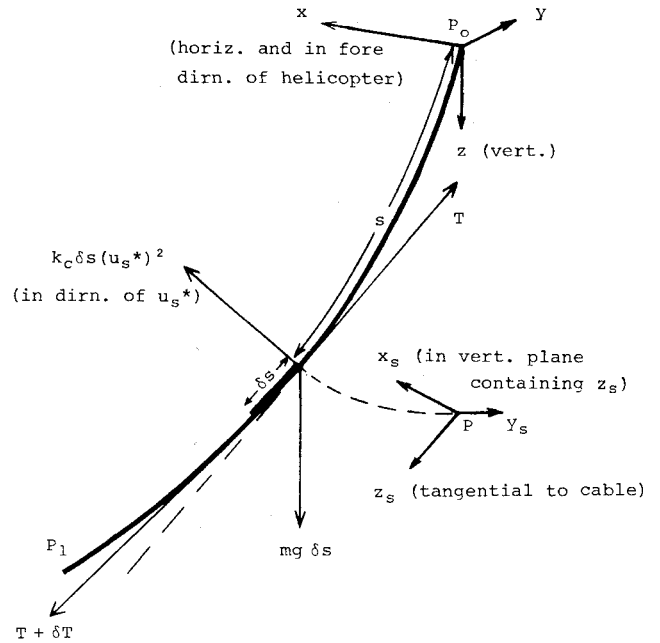


Fig. 1 Forces acting on cable element (all axes system are right-handed orthogonal).

where the pitch angle  $\gamma$  is given directly by Eq. (1c), and the yaw angle  $\chi$  is given by

$$\tan \chi = \cos \beta / \cos \alpha = -\operatorname{cosec} \theta \tan \phi \quad (2)$$

Earth axes serve only to define the separate cable and fluid motions with respect to Earth. For the motion of fluid relative to the cable required here, cable axes are used. It should be noted though that because of the invariance with time of the cable and fluid motion, the  $x_E$ ,  $y_E$ , and  $z_E$  directions are always the same as the respective  $x$ ,  $y$  and  $z$  directions.

On resolving in cable element axes and neglecting second order and higher order differences, the equilibrium equation of an element may be written in vector form as<sup>8</sup>

$$\begin{bmatrix} T \delta \theta \cos \phi \\ -T \delta \phi \\ \delta T \end{bmatrix} + k_c \delta s u_s^* \begin{bmatrix} u_s \\ v_s \\ w_s \end{bmatrix} + mg \delta s \begin{bmatrix} -\sin \theta \\ \cos \theta \sin \phi \\ \cos \theta \cos \phi \end{bmatrix} = \begin{bmatrix} 0 \\ 0 \\ 0 \end{bmatrix} \quad (3)$$

In Eq. (3), the components of the velocity of the fluid relative to the cable in cable element axes are given by

$$\begin{bmatrix} u_s \\ v_s \\ w_s \end{bmatrix} = \begin{bmatrix} u \cos \theta \\ u \sin \theta \sin \phi + v \cos \phi \\ u \sin \theta \cos \phi - v \sin \phi \end{bmatrix} \quad (4)$$

where  $u = u_F - u_H$  and  $v = v_F - v_H$ . The magnitude and direction of the velocity of the fluid relative to the cable are defined by

$$u^* = (u^2 + v^2)^{1/2} \quad (5a)$$

$$\psi = \arctan(v/u) \quad (5b)$$

with corresponding definitions when the above variables are subscripted. Since skin friction is ignored, the velocity component  $w_s$  is not required and is therefore set equal to zero.

In the limit, as  $\delta s$  tends to zero, and using Eq. (1c) to change the independent variable from  $s$  to  $z$ , Eq. (3) may be expressed

in differential form as

$$\frac{d\theta}{dz} = \frac{mg \sin\theta - k_c u_s^* u_s}{T \cos\theta \cos^2\phi} \quad (6a)$$

$$\frac{d\phi}{dz} = \frac{mg \cos\theta \sin\phi + k_c u_s^* v_s}{T \cos\theta \cos\phi} \quad (6b)$$

$$\frac{dT}{dz} = -mg \quad (6c)$$

which are the basic equilibrium equations used here.

For a given sonar system, it is assumed that the cable parameters  $mg$  and  $k_c$  are known in both air and sea. Then, if the motion of the surrounding fluid relative to the cable is known, we can solve Eqs. (6) and establish the cable shape. While hovering above the sea, the helicopter normally heads into wind and both the speed of the helicopter relative to ground and wind speed relative to helicopter are usually given by the helicopter instrumentation. It is assumed, therefore, that these quantities are given† and that no further data about the air and sea environment are measured or known. However, to solve the preceding equations, the velocity components need to be specified fully as functions of  $z$ . A mathematical representation of the air and sea must, therefore, be formulated. In the following presentation, subscripts  $A$  and  $W$  replace subscript  $F$  when the fluid is air and water, respectively.

In representing the wind above the sea, it is assumed that wind direction does not vary with altitude and that the helicopter heads into wind. This results in  $\psi_A = \psi_{A0} = \pm 180$  deg. Generally, conditions above the sea are very difficult to predict and a number of different velocity functions are possible for various stability classifications.<sup>9</sup> The influence of the rotor downwash complicates the airflow even further. In view of these uncertainties, a mathematically complex function is not warranted.

Two commonly used wind profiles, known as power and log laws, are assumed here and defined later. The log law profile is as used for the neutral stability classification.<sup>9</sup> The quantity  $h$  is the known height of  $P_0$  above the sea (i.e., hover height), and  $u_{A0}$  is the known wind speed at  $P_0$  (i.e., the helicopter) relative to ground.

1) Power law:

$$u_A = u_{A0} (1 - z/h)^{1/n} \quad (7)$$

where  $n = 6$  is commonly assumed.

2) Log law:

$$u_A = u_{A0} \ln \{ c - (c-1)z/h \} / \ln c \quad (8)$$

where  $c = 1 + h/h_0$  (Ref. 9, p. 140;  $h_0 = 2.5 \times 10^{-4}$  m for calm sea,  $h_0 = 4.0 \times 10^{-5}$  m for rough sea).

Equations (7) and (8) give very similar wind profiles provided the appropriate values for  $n$  and  $c$  are chosen.

Like winds above the sea, sea currents are extremely difficult to predict. The classical Ekman spiral provides a mathematically convenient function that is fairly realistic for deep water, i.e., particularly for oceans.<sup>10</sup> The magnitude and direction of the spiral is defined for the Southern Hemisphere (For the Northern Hemisphere,  $\psi_w = -3\pi/4 + \pi z/d$ ) and with

$\psi_A = \pm 180$  deg by

$$u_w^* = u_{w0}^* e^{-\pi z/d} \quad (9a)$$

$$\psi_w = 3\pi/4 - \pi z/d \quad (9b)$$

where  $d$  is the depth of frictional resistance,  $u_{w0}^*$  is the water velocity at  $P_0$  (i.e., surface velocity), and  $\psi_w$  is in radians. Equations (9) may be expressed in component form as

$$u_w = u_w^* \cos\psi_w = u_{w0}^* e^{-\pi z/d} \cos(3\pi/4 - \pi z/d) \quad (10a)$$

$$v_w = u_w^* \sin\psi_w = u_{w0}^* e^{-\pi z/d} \sin(3\pi/4 - \pi z/d) \quad (10b)$$

At the sea surface, the direction of the current is 45 deg to the left (right in the Northern Hemisphere) of the wind direction. At the depth of friction, i.e., when  $z = d$ , the water velocity is 0.043 times the surface velocity. The significance attached to the depth  $d$  is that below it, the velocity is considered negligible.

It is assumed that the quantities  $d$  and  $u_{w0}^*$  are not given by any instrumentation. However, empirical expressions for both quantities have been derived. From Refs. 10 and 11, respectively,

$$d \approx 7.6 u_{A0}^* \operatorname{cosec}^{1/2} \phi_E \quad (11a)$$

$$u_{w0}^* \approx 0.03 u_{A0}^* \quad (11b)$$

where  $d$  is in meters for  $u_{A0}$  in meters per second. At latitude  $\phi_E = 35$  deg, Eq. (11a) gives  $d \approx 10 u_{A0}^*$ . References 10 and 11 assume  $u_{A0}^*$  is measured at an altitude of 15 and 10 m, respectively. For the assumed wind profiles,  $u_{A0}^*$  does not vary significantly with altitude in the range expected for a hovering helicopter during sonar operation, i.e., roughly, 10-30 m. Hence, adjustment to the preceding formulae is not warranted for changes in altitude within this range.

In Ref. 10, at wind velocities below about 6 m/s, Eq. (11a) is replaced by

$$d \approx 3.67 (u_{A0}^*)^{3/2} \operatorname{cosec}^{1/2} \phi_E \quad (11c)$$

which, at  $\phi_E = 35$  deg, gives  $d \approx 4.8 (u_{A0}^*)^{3/2}$ . However, this further refinement is not considered necessary in view of the limited confidence in the model of the sea current. Because the angular deviation of the cable is roughly proportional to the square of the velocity (see below), errors are minimized over a large range of velocity by choosing the empirical relation given by Eq. (11a), which is more appropriate for higher velocities. Neither relation allows a meaningful estimate for  $d$  at the equator, i.e., at  $\phi_E = 0$ .

Since the velocity components are now fully specified in both air and sea, it is possible to solve the preceding equilibrium equations.

### Solution of Equilibrium Equations

To obtain a solution of Eqs. (6), Eq. (6c) is first integrated between  $P$  and  $P_I$  (where  $z = z_I$  and  $T = T_I$ ), to give

$$T = T_I - mg(z - z_I) \quad (12)$$

The dimensionless quantities  $\mu = mgz_I/T_I$ ,  $X = x/z_I$ ,  $Y = y/z_I$ ,  $Z = z/z_I$ ,  $S = s/z_I$ , and  $U^* = (k_c z_I/T_I)^{1/2} u^*$  [similarly for all velocities, e.g.,  $V = (k_c z_I/T_I)^{1/2} v$ ] are now introduced with the subscripts already used retaining their meaning. On substituting for  $T$  from Eq. (12), Eqs. (6a and b) may be written in terms of the dimensionless quantities as

$$\frac{d\theta}{dZ} = \frac{\mu \sin\theta - U_s^* U_s}{[1 - \mu(Z - 1)] \cos\theta \cos^2\phi} \quad (13a)$$

†Wind speed at the helicopter relative to ground is readily obtained from these quantities.

$$\frac{d\phi}{dZ} = \frac{\mu \cos\theta \sin\phi + U_s^* V_s}{[1 - \mu(Z-1)] \cos\theta \cos\phi} \quad (13b)$$

Given  $\theta = \theta_1$  and  $\phi = \phi_1$  at  $P_1$ , the above pair of simultaneous linear differential equations must be solved in order to obtain the angles  $\theta = \theta_0$  and  $\phi = \phi_0$  at  $P_0$ , where  $Z = 0$ . Knowing the angles  $\theta$  and  $\phi$ , the cable shape can be evaluated readily by numerical integration of Eqs. (1).<sup>8</sup>

For the velocity functions assumed, Eqs. (13) can only be solved numerically. However, an analytical solution is possible for the two-dimensional case in a uniform flowfield.<sup>2,8</sup> This case was therefore used to check the accuracy of the numerical method used (Runge-Kutta second order).

In order that solutions can be obtained for any specific case more readily, further approximations are now made. These enable analytical solutions that require minimal reference to numerically derived results. It is therefore assumed that 1) the effective cable mass is concentrated at  $P_1$ , the lower end of the cable length, and 2) angles  $\theta$  and  $\phi$  are sufficiently small to allow the usual small angle approximations. The former assumption requires  $\mu$  to be set equal to zero in Eqs. (13) and  $T_1$  to be replaced by  $T_1(1 + \mu)$ . Because  $T_1$  is used in defining the nondimensional velocity magnitude and components, this replacement has the effect of multiplying the velocities by  $(1 + \mu)^{-1/2}$ . Using the small angle approximations, Eqs. (13) may then be written as<sup>8</sup>

$$\frac{d\theta}{dZ} = \frac{-U^* U}{(1 + \mu)} \quad (14a)$$

$$\frac{d\phi}{dZ} = \frac{U^* V}{(1 + \mu)} \quad (14b)$$

where the tension along the cable is constant and is given by

$$T = T_1(1 + \mu) \quad (15)$$

On integrating between  $P$  and  $P_1$ ,

$$\theta = \theta_1 + \frac{1}{(1 + \mu)} \int_Z^1 U^* U dZ \quad (16a)$$

$$\theta = \theta_1 - \frac{1}{(1 + \mu)} \int_Z^1 U^* V dZ \quad (16b)$$

where the angles  $\theta = \theta_0$  and  $\phi = \phi_0$  at  $P_0$  are given by setting  $Z = 0$ . Eqs. (16) provide an analytical three-dimensional solution only when the fluid velocity is uniform or is suitably chosen such that the integrations can be performed analytically.

For the uniform velocity case, Eqs. (16) give

$$\theta = \theta_1 + U_0^* U_0 (1 - Z) / (1 + \mu) \quad (17a)$$

$$\phi = \phi_1 + U_0^* V_0 (1 - Z) / (1 + \mu) \quad (17b)$$

The cable shape may readily be obtained analytically using the small angle approximations.<sup>8</sup>

The validity of the preceding "approximate" solutions was determined by comparing them with appropriate "general" solutions for both two- and three-dimensional cases.<sup>8</sup> An example of a comparison for the latter case is given in Fig. 2. Where angular deviations from the vertical are small and the weight of the cable is significantly less than the applied tension at the lower end (usually for small values of the parameters  $\mu$ ,  $\gamma_1$ , and  $U_0^*$ ), agreement is observed to be good.

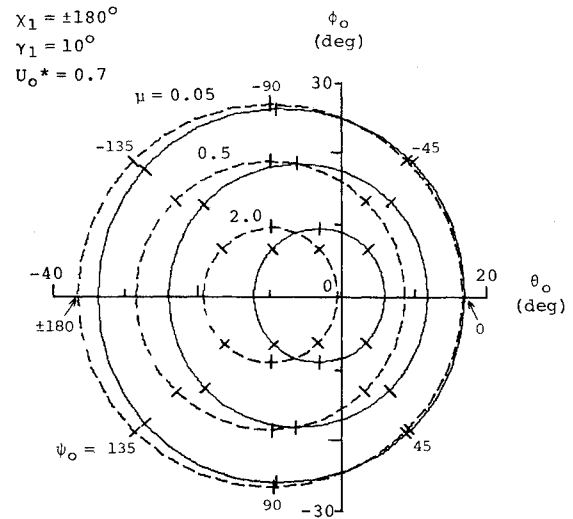


Fig. 2 Comparison between three-dimensional "general" (full line) and "approximate" (broken line) solution of angular orientation in pitch and roll for uniform fluid velocity, parameter  $\mu$ , and independent variable  $\psi_0$ . Tick marks indicate equispaced values of  $\psi_0$ .

For the case of a nonuniform fluid velocity, a procedure is now developed whereby the nonuniform velocity is replaced by an equivalent uniform one so that the analytical solution given by Eqs. (17) may be used. In general, these equivalent values are determined numerically using Simpson's formula, but once derived, separate analytical solutions are possible for all parameter values appropriate to the uniform velocity case. This allows a more compact presentation of results as only these equivalent values need to be shown for each velocity profile. Following its derivation, the procedure is then applied to the wind and sea representation assumed earlier.

Equivalent values of the mean fluid velocity components  $U_F$  and  $V_F$  are defined to be those values which give the same solution of Eqs. (16) at  $Z = 0$  as obtained when the actual nonuniform values are used. This requires

$$\langle U^* \rangle \langle U \rangle = \int_0^1 U^* U dZ \quad \langle U^* \rangle \langle V \rangle = \int_0^1 U^* V dZ \quad (18)$$

where all variables enclosed by " $\langle \rangle$ " and " $\langle \rangle$ " are mean values. Nondimensional velocities are now scaled by  $U_{F0}^*$  (assumed nonzero), the value of  $U_F^*$  at  $P_0$ , to give  $\omega = U_F^* / U_{F0}^*$ ,  $\lambda = U_H^* / U_{F0}^*$ , and  $\sigma = U^* / U_{F0}^*$  with  $x$  and  $y$  components denoted by subscripts  $x$  and  $y$ , respectively. Assuming the scaled nondimensional fluid velocity components  $\omega_x$  and  $\omega_y$  are known functions of  $Z$ , equivalent mean values  $\langle \omega_x \rangle$  and  $\langle \omega_y \rangle$  may be derived. Corresponding nonscaled values  $\langle U_F \rangle$  and  $\langle V_F \rangle$  are obtained by multiplying by  $U_{F0}^*$ . Since  $\lambda_x$  and  $\lambda_y$  are constant,  $\langle \sigma_x \rangle = \langle \omega_x \rangle - \lambda_x$  and  $\langle \sigma_y \rangle = \langle \omega_y \rangle - \lambda_y$ . Equations (18) may, therefore, be expressed in terms of these scaled variables as<sup>8</sup>

$$(\langle \sigma_x \rangle^2 + \langle \sigma_y \rangle^2)^{1/2} \langle \sigma_x \rangle = \beta_x \quad (19a)$$

$$(\langle \sigma_x \rangle^2 + \langle \sigma_y \rangle^2)^{1/2} \langle \sigma_y \rangle = \beta_y \quad (19b)$$

where

$$\beta_x = \int_0^1 U^* U dZ = \int_0^1 (\sigma_x^2 + \sigma_y^2)^{1/2} \sigma_x dZ$$

$$\beta_y = \int_0^1 U^* V dZ = \int_0^1 (\sigma_x^2 + \sigma_y^2)^{1/2} \sigma_y dZ$$

Equations (19) may be solved for  $\langle \omega_x \rangle$  and  $\langle \omega_y \rangle$  to give

$$\begin{aligned} \langle \omega_x \rangle &= \lambda_x + \{ |\beta_x| (1 + \beta_y^2 / \beta_x^2)^{-1/2} \}^{1/2} |\beta_x| / \beta_x \quad \text{for } \beta_x \neq 0 \\ &= \lambda_x \quad \text{for } \beta_x = 0 \end{aligned} \quad (20a)$$

$$\begin{aligned} \langle \omega_y \rangle &= \lambda_y + \{ |\beta_y| (1 + \beta_x^2 / \beta_y^2)^{-1/2} \}^{1/2} |\beta_y| / \beta_y \quad \text{for } \beta_y \neq 0 \\ &= \lambda_y \quad \text{for } \beta_y = 0 \end{aligned} \quad (20b)$$

When the velocity of the fluid relative to the cable is two-dimensional, in the  $xz$  plane, Eqs. (19) reduce to

$$|\langle \sigma_x \rangle| \langle \sigma_x \rangle = \beta_x \quad (21)$$

where

$$\beta_x = \int_0^1 |\sigma_x| \sigma_x dZ$$

which gives

$$\begin{aligned} \langle \omega_x \rangle &= \lambda_x + |\beta_x|^{3/2} / \beta_x \quad \text{for } \beta_x \neq 0 \\ &= \lambda_x \quad \text{for } \beta_x = 0 \end{aligned} \quad (22)$$

When the velocity of the fluid relative to the cable is three-dimensional, it is often convenient (see below) to assume that for the purpose of obtaining equivalent mean fluid velocity components  $\langle \omega_x \rangle$  and  $\langle \omega_y \rangle$ , the  $x$  and  $y$  components of the relative fluid velocity can be treated independently. Then Eq. (22) may be used to obtain  $\langle \omega_x \rangle$ , and a corresponding equation in the  $y$  direction may be used to obtain  $\langle \omega_y \rangle$ . Rewriting Eq. (19a) in the form

$$|\langle \sigma_x \rangle| \sigma_x (1 + \langle \sigma_y \rangle^2 / \langle \sigma_x \rangle^2)^{1/2} = \int_0^1 |\sigma_x| \sigma_x (1 + \sigma_y^2 / \sigma_x^2)^{1/2} dZ \quad (23)$$

it can be seen that by replacing  $\sigma_x$  and  $\sigma_y$  by  $\langle \sigma_x \rangle$  and  $\langle \sigma_y \rangle$ , respectively, only in the square root term of the integrand, this equation reduces to Eq. (21). A similar result may be obtained from Eq. (19b) for the  $y$  direction. If, over the range of integration, the variation of  $(1 + \sigma_y^2 / \sigma_x^2)^{1/2}$  is high, the approximation may be poor. It should be noted that this independent treatment of the velocity components (referred to as independent velocity component assumption) is confined to the calculation of equivalent mean fluid velocity components; uniform velocity three-dimensional formulae should be used to obtain angular deviations in pitch and roll.

The equivalent mean fluid velocity procedure is now applied to the assumed models of the wind and sea.

#### Winds above the Sea

For the wind profiles, the velocity of the fluid relative to the cable is two-dimensional provided any helicopter motion is in the same direction as the wind (i.e.,  $\psi_H = 0$  or  $\pm 180$  deg, or  $\lambda_y = 0$ ); otherwise, the relative velocity is three-dimensional. Using the equivalent mean fluid velocity concept for the two-dimensional case,  $\langle \omega_y \rangle = 0$  and  $\langle \omega_x \rangle$  is readily given by Eq. (22). However, for the three-dimensional case,  $\langle \omega_x \rangle$  and  $\langle \omega_y \rangle$  should be recalculated for each value of  $\lambda_y$ . It is, therefore, convenient to use the independent velocity component assumption outlined previously. Then, for a given value of  $\lambda_x$ , the values  $\langle \omega_x \rangle$  and  $\langle \omega_y \rangle$  remain unchanged for all values of  $\lambda_y$ . For the wind profiles assumed, using typical parameter values experienced, this approximation was generally found to be good when  $|\lambda_y|$  was reasonably small, i.e., less than about 0.5. This is to be expected since, for small  $\lambda_y$ ,  $(1 + \sigma_y^2 / \sigma_x^2)^{1/2}$ , which equals  $\{1 + \lambda_y^2 / (\omega_x - \lambda_x)^2\}^{1/2}$ , does

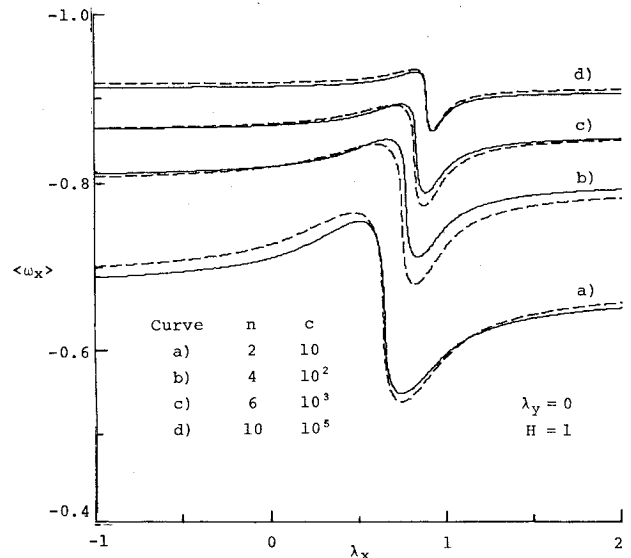


Fig. 3 Equivalent mean fluid velocity for power (full line) and log (broken line) laws;  $\langle \omega_x \rangle$  vs  $\lambda_x$  for parameters  $n$  or  $c$ .

not differ significantly from unity throughout most of the range of integration for both profiles.

Analytical solutions for  $\langle \omega_x \rangle$  from Eq. (22) are possible. However, they are given by lengthy formulae so that, except for special cases, results were obtained by integrating numerically using Simpson's formula. For the special case when  $\lambda_x = 0$  and  $H = h/z_I = 1$ ,<sup>†</sup> from Eq. (22),  $\langle \omega_x \rangle$  is given analytically for the power law by

$$\langle \omega_x \rangle = - \left[ \int_0^1 (1 - Z)^{2/n} dZ \right]^{1/2} = - \left[ \frac{n}{2+n} \right]^{1/2} \quad (24)$$

and for the log law by

$$\begin{aligned} \langle \omega_x \rangle &= - \left[ \int_0^1 \frac{\ln^2 \{ c - (c-1)Z \}}{\ln^2 c} dZ \right]^{1/2} \\ &= - \left[ \frac{c}{c-1} \left( 1 - \frac{2}{\ln c} \right) + \frac{2}{\ln^2 c} \right]^{1/2} \end{aligned} \quad (25)$$

Figure 3 shows the variation of  $\langle \omega_x \rangle$  with  $\lambda_x$  at  $H = 1$  and  $\lambda_y = 0$  for a range of parameter values  $n$  and  $c$ . Pairs of the parameters have been suitably chosen to give similar profiles when each parameter is used in the appropriate law. The sudden change in  $\langle \omega_x \rangle$  observed for each curve is produced by the effect of a reversal in the fluid drag force along the cable, i.e.,  $\sigma_x$  changes sign. For the usual case of a submerged sonar body, and using the independent velocity component assumption, the solution for  $\theta_0$  and  $\phi_0$  is then readily obtained from values of  $\langle \omega_x \rangle$  given by Fig. 3. This is achieved on setting  $U_0 = U_{A0}^* (\langle \omega_x \rangle - \lambda_x)$  and  $V_0 = -U_{A0}^* \lambda_y$  in Eqs. (17).

#### Sea Currents

During normal sonar operation, it is generally desirable for the sonar body to remain vertical. For the mathematical model used here, this requires (for  $\gamma_I = 0$ ) the relative fluid velocity at the body to be zero, i.e.,  $\lambda_x = \omega_{xI}$  and  $\lambda_y = \omega_{yI}$ , where  $\omega_{xI}$  and  $\omega_{yI}$  are the values of  $\omega_x$  and  $\omega_y$ , respectively, at  $P_I$ . Equivalent mean fluid velocities, which are obtained by integrating numerically using Simpson's formula, are, therefore, presented assuming this condition.

In Fig. 4, both the Ekman spiral and equivalent mean fluid velocity are shown in the  $xy$  plane as functions of  $Z/D$  and

<sup>†</sup> $H$  always equals one when the sonar body is submerged.

$1/D$  respectively, where  $D=d/z_l$ . Equivalent mean fluid velocity values calculated using the independent velocity component assumption are compared with the values obtained without this assumption, i.e., using Eqs. (20).

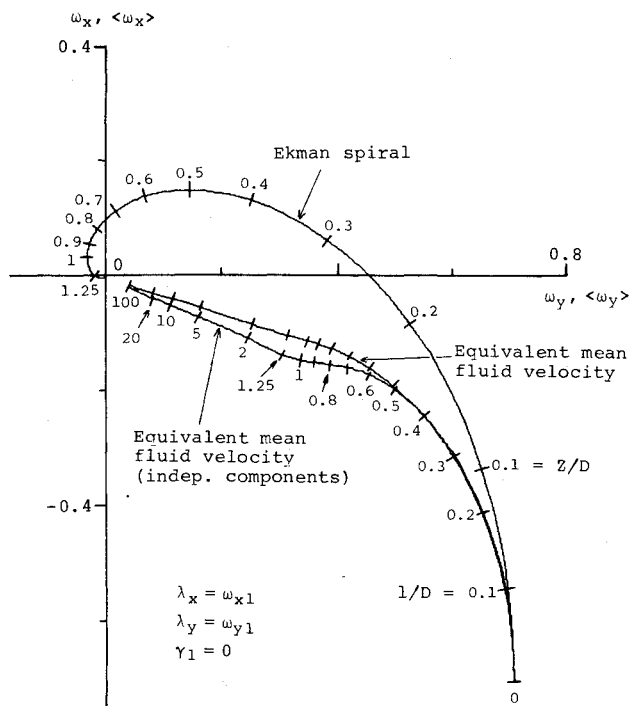


Fig. 4 Ekman spiral ( $\omega_x, \omega_y$ ) and equivalent mean fluid velocity ( $\langle \omega_x \rangle, \langle \omega_y \rangle$ ), for independent variables  $Z/D$  and  $1/D$ , respectively (values shown beside tick marks). Equivalent mean fluid velocity calculated using independent velocity component assumption is also shown.

Agreement is seen to be very good for the lower and upper range of values of  $1/D$  shown. As explained above, regions of good agreement imply there is only small variation in the term  $(1 + \sigma_y^2 / \sigma_x^2)^{1/2}$  throughout the range of integration. The absolute error in the approximate values is given by the distance between points on the two mean velocity curves of Fig. 4 which have the same value of  $1/D$ . This error is a maximum of 0.037 at  $1/D \approx 1.05$  and is about 0.01 at  $1/D = 0.6$  and 14. Although these errors are much larger than those generally experienced when considering winds above the

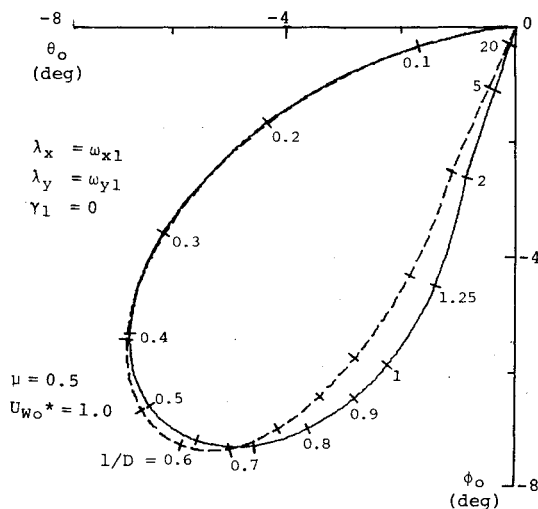


Fig. 5 Three-dimensional "approximate" solution (full line) of angular orientation in pitch and roll for Ekman spiral with independent variable  $1/D$  (values shown beside tick marks). Solution is also shown (broken line) using independent velocity component assumption.

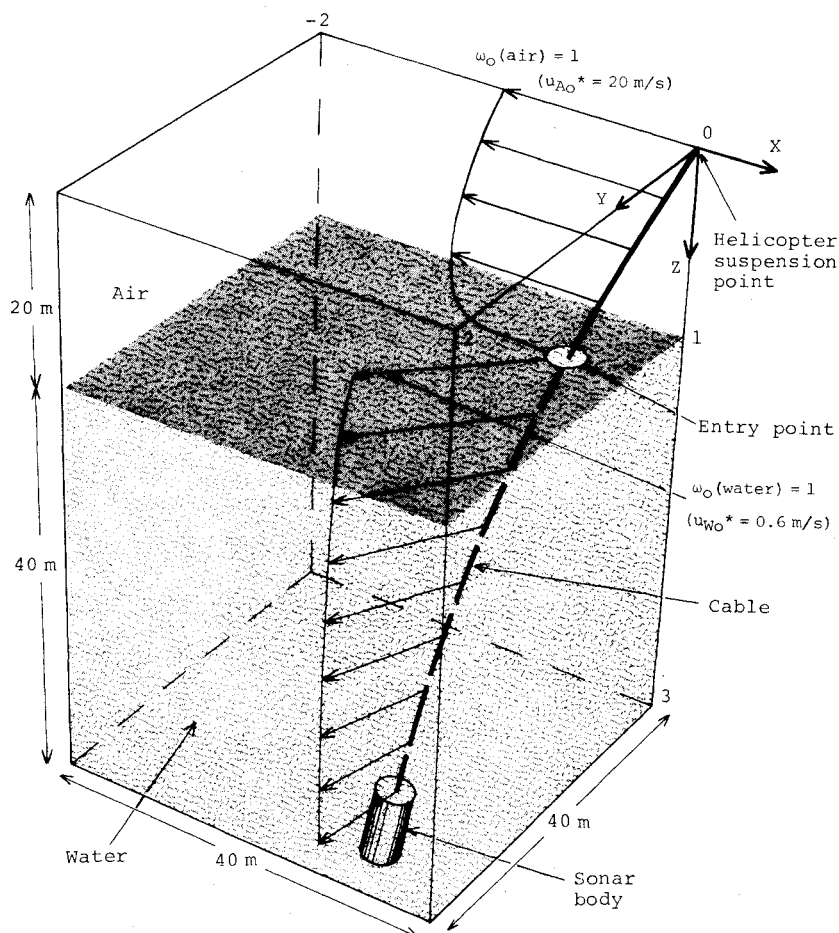


Fig. 6 Example of sonar body suspended from a helicopter; note the difference in scales of the fluid velocity vectors for air and water.

sea, they may well be acceptable when viewed in relation to uncertainties already existing.

For the sonar body at a specified depth, the values of  $\langle \omega_x \rangle$  and  $\langle \omega_y \rangle$  given by Fig. 4 then enable solutions for  $\theta_0$  and  $\phi_0$  to be obtained for the cable length in air. For a specific case, solutions of angular orientation in pitch and roll are given in Fig. 5 and are compared with solutions obtained using the "independent component" equivalent mean fluid velocities. Errors are seen to correspond to those observed in Fig. 4. Results obtained from the "general" solution are not shown since they were found to agree very closely with the "approximate" solution results (i.e., full lines of Fig. 5). Good agreement is to be expected because the angular deviations from the vertical are small.

#### Example of Sonar Body Suspended from a Helicopter

So far, solutions have been presented only for a length of cable totally immersed in a single Newtonian fluid. However, the main case of interest in this study is of a sonar body suspended from a helicopter. Here, the cable passes through two fluid layers (air and water) and the method of approach outlined at the beginning should be used. The method could easily be extended to any number of fluid layers. Using a power law for the wind above the sea, and an Ekman spiral for the sea current, an example is given below in which cable orientation and shape are determined from the general equations [i.e., Eqs. (13)] without using the approximations that enable an analytical solution.

Constants that are independent of the fluid are  $g = 9.81 \text{ m/s}^2$ ,  $d_c = 20 \text{ mm}$ ,  $C_D = 1.2$ , and  $u_H^* = 0$ .

The assumed conditions in air are  $\rho A = 1.226 \text{ kg/m}^3$ ,  $mg = 6.2 \text{ N/m}$ ,  $z_l = h = 20 \text{ m}$  (i.e.,  $H = h/z_l = 1$ ),  $u_{A0}^* = 20 \text{ m/s}$ ,  $\psi_A = \pm 180 \text{ deg}$ , and  $n = 6$  (for power law).

The assumed conditions in water are  $\rho w = 1023 \text{ kg/m}^3$ ,  $T_l = 60 \text{ N}$ ,  $z_l = 40 \text{ m}$ ,  $d = 10 u_{A0}^* = 200 \text{ m}$  (i.e.,  $D = d/z_l = 5$ ),  $u_{w0}^* = 0.03 u_{A0}^* = 0.6 \text{ m/s}$ ,  $\gamma_l = 20 \text{ deg}$ ,  $\chi_l = \psi_l = (0.75\pi - \pi D) \text{ rad} = 99 \text{ deg}$  (i.e., at attached body, cable is inclined in a vertical plane in the flow direction), and  $mg = 3.0 \text{ N/m}$  [obtained by subtracting the upthrust,  $\rho_w g (\frac{1}{2} \pi d_c^2)$ , from the value of  $mg$  in air].

In water, using Eq. (12),  $T_0 = T_l + mgz_l = 180 \text{ N}$ , which is equal to  $T_l$  in air. The dimensionless quantities  $\mu$  and  $U_0^*$  are then calculated for both air and water. In air,  $\mu = 0.69$  and  $U_0^* = 0.81$ ; in water,  $\mu = 2.0$  and  $U_0^* = 1.72$ .

On numerically solving the general equations, cable orientation and linear displacement coordinates are obtained. Figure 6 illustrates the cable shape together with the horizontal fluid velocity vectors. For each fluid, these vectors represent the scaled velocity  $\omega$ , where  $\omega_0 = 1$ . All displacement coordinates are expressed in terms of dimensionless coordinates for the cable in air and should be multiplied by 20 to give displacement in meters. Values of  $(\theta, \phi)$  obtained are  $(-3.3, -19.7 \text{ deg})$  at sonar body,  $(-17.5, -29.0 \text{ deg})$  at sea surface, and  $(-26.3, -14.5 \text{ deg})$  at helicopter.

### Concluding Remarks

Although the three-dimensional steady-state mathematical model derived is intended to represent a cable used to suspend a sonar body from a helicopter, the dimensionless form of presentation allows application to a number of practical cable problems. The general cable equilibrium equations can only be solved numerically. However, following various approximations, a three-dimensional analytical solution is possible for a uniform fluid velocity. The solution is found to be suitable when angular deviations of the cable from the vertical are small. For a nonuniform fluid velocity, and when the weight of the cable is significantly less than the applied tension at the lower end, the solution may be simplified by replacing the velocity function by an equivalent mean value so that the "approximate" analytical solution for a uniform fluid velocity may be used. This procedure of calculating an equivalent value would also be very useful for simplifying the representation of the environment in developing a mathematical model for a flight simulator.

### Acknowledgment

The author is indebted to G.D. Mallinson for use of his graphics computer programs, which were used to obtain views of three-dimensional images.

### References

- <sup>1</sup>Packer, T.J., "Wessex Helicopter/Sonar Dynamics Study. The Mathematical Model of the Sonar Cable and Transducer," Weapons Research Establishment, Salisbury, South Australia, WRE Rept. 951 (WR & D), May 1973.
- <sup>2</sup>Glauert, H., "The Form of a Heavy Flexible Cable Used for Towing a Heavy Body below an Aeroplane," Aeronautical Research Committee, R&M 1592, 1934.
- <sup>3</sup>Landweber, L. and Protter, M.H., "The Shape and Tension of a Light Flexible Cable in a Uniform Current," *Journal of Applied Mechanics, Transactions of ASME*, Vol. 14, 1947, pp. 121-126.
- <sup>4</sup>Neumark, S., "Equilibrium Configurations of Flying Cables of Captive Balloons, and Cable Derivatives for Stability Calculations," Aeronautical Research Council, London, R&M 3333, June 1961.
- <sup>5</sup>Eames, M.C., "Steady-State Theory of Towing Cables," Naval Research Establishment, Canada, DREA Rept. 67/5, 1967.
- <sup>6</sup>Genin, J. and Canon, T.C., "Equilibrium Configuration and Tensions of a Flexible Cable in a Uniform Flowfield," *Journal of Aircraft*, Vol. 4, May-June 1967, pp. 200-202.
- <sup>7</sup>Duncan, W.J., *The Principles of the Control and Stability of Aircraft*, Cambridge University Press, London, 1959, p. 79.
- <sup>8</sup>Gilbert, N.E., "Steady State Behaviour of a Cable Used for Suspending a Sonar Body from a Helicopter," Aeronautical Research Laboratories, Melbourne, Australia, ARL Aero Rept. 149, May 1978.
- <sup>9</sup>Roll, H.U., *Physics of the Marine Atmosphere*, Academic Press, N.Y., 1965.
- <sup>10</sup>Sverdrup, H.U., Johnson, M.W., and Flemming, R.H., *The Oceans*, Prentice Hall, N.Y., 1946.
- <sup>11</sup>Spillane, K.T., "Movement of Oil on the Sea Surface," *Australian Meteorology Magazine*, Vol. 19, Dec. 1971, pp. 158-177.